

Prediction Model of Residual Current Based on Grey Association and Neural Network

Guoyu Sun*

School of Automation, Harbin University of Science and Technology,
No. 52, Xuefu Road, Nangang District, Harbin City, Heilongjiang Province 150080, China

(Received November 30, 2023; accepted March 6, 2024)

Keywords: electrical fire warning, grey association, neural network, prediction model

To enhance early electrical fire warning in power IoT systems, we propose a residual current modeling method combining grey correlation and neural networks. By analyzing 27985 sets of data from an intelligent fire monitoring system, effective data collection and processing with advanced sensor technology in an IoT context were demonstrated. The model, derived from correlation analysis and grey prediction algorithms, uses a trained neural network for predicting residual current. This method not only augments the efficiency and accuracy of data processing in IoT but also underscores the significance of sensor technology in electrical monitoring and fire prevention. The comparative analysis of predicted and actual residual currents, showing an error range of 0.18 to 3.21%, validates the accuracy of the model and the utility of sensor-driven methods in IoT applications.

1. Introduction

The occurrence of fires caused by electrical faults has increased considerably in recent years. Data from 2014 to 2018 indicate that out of 8875 fires in Shenzhen, China, 3192 were electrical fires, making up 35.97% of the total number of incidents. These fires led to 21 fatalities and 35 injuries, inflicting direct economic damage of approximately 53.901 million yuan.⁽¹⁾ Significantly, electrical fires in residential and dormitory structures constituted a substantial proportion of the overall count, casualties, and financial losses. Specifically, residential electrical fires represented 54.98% of these incidents and were responsible for nearly 23.87% of the total economic loss due to electrical fires.⁽²⁾

To mitigate the risk of electrical fires, the installation of arc fault detection devices (AFDDs) has been widely adopted both domestically and internationally.⁽³⁾ While advancements in AFDD technology are observed, challenges related to false alarms and undetected faults remain. Concerns regarding the longevity of the device and its substantial cost have also been raised. Consequently, research into electrical fire early warning technology is deemed necessary. Owing to advancements in information and sensing technologies, the integration of multisensor data for fire alarms has been identified as an emerging industry trend. By this technique, the

*Corresponding author: e-mail: sungy618@163.com
<https://doi.org/10.18494/SAM4784>

parameters detected by various sensors, such as temperature, smoke concentration, and carbon monoxide levels, are synthesized to evaluate the potential and intensity of fires.^(4–7) Methods and algorithms pertinent to this topic have been proposed by several scholars. An early warning algorithm for indoor fires, based on a backpropagation neural network and integrated temperature, smoke, and carbon monoxide data to estimate fire likelihood, was introduced.⁽⁸⁾ We enhanced the distinction between fire signals and environmental disturbances by applying nonuniform sampling and trend extraction techniques. A strategy to refine fire detection precision and reliability using the long short-term memory network and environmental data fusion was previously presented.⁽⁹⁾ A recommendation for employing a fiber optic distributed temperature sensing system in conjunction with a deep anomaly detection model for early fire heat release monitoring has also been put forward.⁽¹⁰⁾ A smart building fire detection system leveraging artificial intelligence and multisensor fusion has also been designed.⁽¹¹⁾ However, it was observed that the prevailing techniques predominantly issue warnings after fire inception, indicating a deficiency in preventive measures. Among the catalysts for electrical fires, residual current is identified as a principal factor contributing to these incidents. When the insulating material sustains damage due to aging, physical damage, overheating, or chemical corrosion, its ability to effectively isolate current is compromised. Under such circumstances, current leakage may occur, implying that the current does not flow along the predetermined path but may instead divert to combustible materials in proximity to the conductor, thereby posing a fire risk. This situation causes the generation of voltage and current from residual currents, leading primarily to ground faults, notably short circuits between phase wires and grounded conductive bodies, as depicted in Fig. 1.

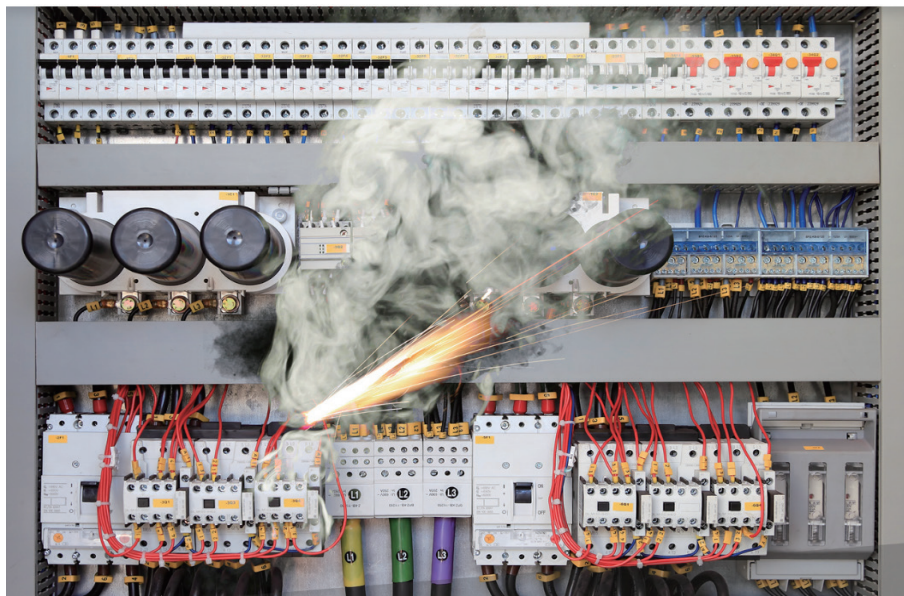


Fig. 1. (Color online) Fire caused by electrical short circuit.

On the basis of available statistics, it is estimated that 90% of fires attributed to electrical short circuits arise from ground fault arcing.⁽¹²⁾ Furthermore, while the residual current in a distribution system might not immediately instigate a fire, an observed trend is the progressive increase in this current over time. Prolonged overload or leakage can culminate in distribution line heating, subsequent insulation deterioration, and eventual fire outbreak. The utilization of residual current devices (RCDs) or residual current circuit breakers (RCBOs) with overcurrent protection has been demonstrated to prevent such fires. Various types of fault exist within electrical installations, and certain faults must be present for an RCD/RCBO to effectively prevent or halt a fire. RCDs function by measuring the current balance between two conductors, analogous to a balanced seesaw. For circuits connected to an RCD, the outgoing current should remain balanced with the returning current. When an imbalance arises owing to a fault or if an individual interacts with the circuit, current leakage (typically between 5 and 30 mA) is detected. Subsequently, in less than 300 ms, the RCD severs the supply, averting electrocution. Thus, for an RCD to impede or preclude a fire, circuit imbalance is essential, given that this imbalance triggers the RCD to disconnect the power source. RCDs offer protection against electrocution and a specific type of live-earth fault, potentially culminating in a fire, termed ‘surface tracking’. This phenomenon occurs when mineral deposits from detergents or spillages accumulate around cables, such as in appliances like washing machines or dishwashers. Once a significant amount of deposits form, arcing commences, leading to the aforementioned imbalance, subsequently activating the RCD. However, a majority of electrical fires originate from high-resistance connections (HRCs), inducing excessive heat generation. Circuit breakers, RCDs, and RCBOs typically fail to identify HRCs since they often manifest externally. These faults inherently cause the connections to reach extreme temperatures, exceeding 1000 °C, quickly escalating to a fire. If the power supply remains uninterrupted at this juncture, fire progression becomes challenging to contain. Thus, the prediction of residual currents is recognized as a vital tool for the early prevention of electrical fires.^(13–15)

Existing research indicates that while time series analysis has made some progress in predicting nonlinear data, it still faces challenges in handling the dynamism and complexity of nonlinear data.⁽¹⁶⁾ The uncertainty of nonlinear relationships and sensitivity to initial conditions make predictions more difficult. The long-term historical dependence and complex structure of the data, such as cyclicity and seasonality, necessitate more advanced analytical methods. Therefore, traditional time series methods may be limited in their accuracy and predictive capabilities for nonlinear data.

In Sect. 2, we outline an innovative approach employing a grey neural network model for the analysis and prediction of electrical data, particularly focusing on residual current. This method emphasizes the significance of each input parameter. Distinct from traditional fire alarm technologies, which activate solely during a fire, this approach provides a proactive early warning system through the identification of anomalies in circuit data. The model, utilizing the grey prediction algorithm, demonstrates capability in forecasting output parameter data amidst uncertainty. Integration with the forward neural network algorithm enables the effective handling of nonlinear computations and complex data, facilitating the forecasting of a comprehensive range of expected values. This approach utilizes parameter data for predictive analysis, leading to the generation of predictive outcomes. The resulting early warning system,

based on the predictive values of residual current, significantly reduces fire risks and offers a proactive method for mitigating electrical fires. Integrating IoT and sensor technologies enables continuous monitoring and real-time data analysis, facilitating early detection and intervention, which greatly enhances safety standards in both residential and industrial settings.

2. Smart Electricity Monitoring System

To gather comprehensive power consumption data, a system proficient in the real-time collection and transmission of multisource terminal power consumption data is employed in this study. Continuously active, the system records parameters such as residual current, voltage, and temperature, providing a detailed view of the power consumption dynamics. By integrating these metrics with IoT, anomalies and patterns in the continuous flow of electrical data are identified.⁽¹⁷⁾ In this study, we developed a system that actively mitigates electrical fire risks. Advanced sensors and algorithms enabled us to detect early signs of potential fires, such as unusual heat patterns and electrical irregularities. Our system promptly alerted relevant authorities and occupants, allowing for immediate preventive actions. This approach significantly reduced the likelihood of fire ignition, minimized property damage, and enhanced occupant safety. We developed an advanced power consumption system that actively monitored real-time data and detected irregularities. By analyzing these irregularities, we identified the most likely fault types, providing crucial insights for electrical safety. This system, acting as a digital guardian, continuously assessed and predicted risks in real time, emerging as a key tool in preventing electrical fires and enhancing the durability of power systems.

Figure 2 shows the detailed architecture of the intelligent power consumption system, comprising residual current transformers, electrical fire monitoring hardware, a cloud-based platform, a data center, a PC interface, and a mobile application.

Located centrally within the system, the electrical fire monitoring apparatus is continuously monitored. The electrical activity of power lines is regularly examined, focusing on three primary parameters: voltage, current, and temperature, all recorded in real time. In the course of its regular operation, data is sent by the device to the expansive cloud platform. Subsequently, this data is stored securely in a structured database. When interaction with the system occurs, either through a PC interface or a mobile application, a sequence of processes is initiated. Data is retrieved promptly from the database, enabling a visualization of the recorded information. Nonetheless, the established process is interrupted if anomalous data is detected. An alert is promptly sent to the PC interface and mobile application, and an alarm is activated in response to the identified discrepancy, emphasizing the real-time responsiveness of the intelligent power consumption system.

In Fig. 3, the system modeling flowchart presented in this paper is illustrated. Initially, a correlation analysis of the electrical data was conducted. On the basis of the type of system data, a suitable model and parameters were chosen. Subsequently, a grey prediction model for residual current and the factors affecting it was developed. Given that the factors affecting residual current include parameters unmonitored by the system, and considering the capability of the grey prediction algorithm to forecast data with uncertain factors, the employment of the grey prediction algorithm, in tandem with the optimized neural network combination model, offers

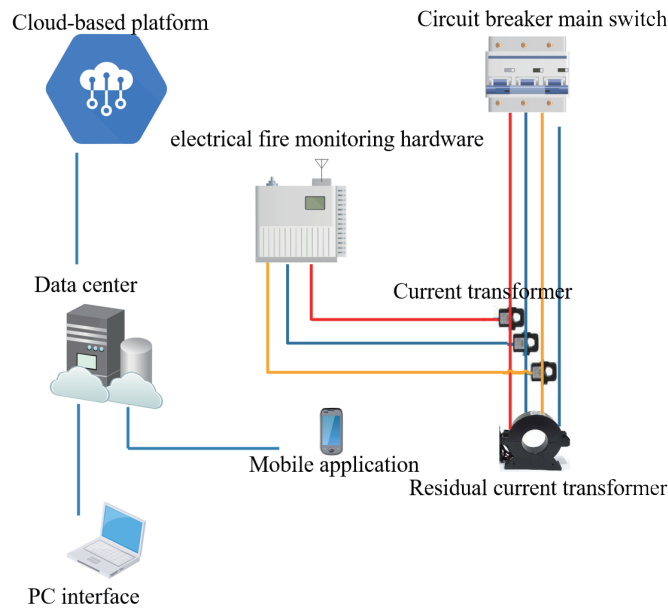


Fig. 2. (Color online) Intelligent power consumption system.

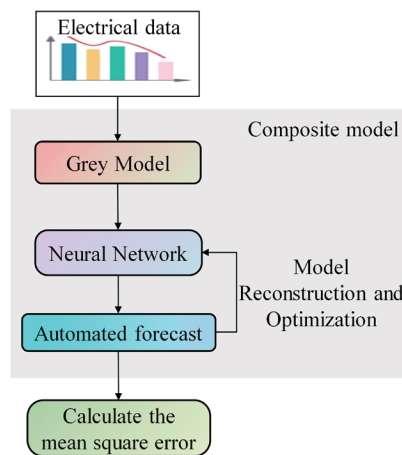


Fig. 3. (Color online) Modeling process of the system.

distinct benefits. Once the data pertaining to the factors affecting the residual current for the predicted period were acquired through grey prediction, the neural network model was trained using historical data. This training was aimed at computing the residual current across all periods. By thoroughly incorporating historical information, the results of the residual current prediction were ascertained. Ultimately, the strengths and weaknesses of the model were assessed through the calculation of its error accuracy.

The modeling and simulation experiment in this study holds significant importance in the field of fire safety, as it explores the potential of smart electricity fire monitoring systems in

preventing and predicting electrical fires, which are crucial for both the electrical industry and public safety. For example, abnormal fluctuations in current or voltage might indicate potential safety risks, while monitoring the temperature of electrical equipment can provide immediate warnings of overheating. Conducted between June 30, 2018 and April 16, 2019, the study involved collecting 27985 sets of electrical data, each encompassing nine monitoring values such as three-phase voltage, A-phase current, temperature, and residual current. The analysis and modeling of such data are key to understanding electrical anomaly patterns that lead to fires. Insights gained from abnormal current or voltage fluctuations and temperature monitoring are instrumental in developing predictive tools to prevent electrical faults, thereby enhancing the design and maintenance strategies of electrical systems and reducing fire risks. The significance of this experiment extends well beyond the technical realm, and the results contribute to broader societal safety and technological advancements in fire prevention. The following is the specific method theory.

2.1 Correlation analysis

Correlation analysis is crucial for understanding how different variables, especially in residual current prediction, are interrelated. It examines the dependences and strengths of their relationships, which is key in identifying factors that significantly impact residual current changes. This understanding enhances the accuracy of predictions and promotes the development of effective monitoring and preventive measures against electrical hazards. Essentially, correlation analysis identifies critical variables for residual current and aids in creating advanced predictive models, leading to improved safety in electrical systems.

The correlation coefficient is based on the deviation of two variables from their respective mean values and is calculated referring to the product-moment correlation coefficient, i.e., the degree of correlation between the two variables is reflected by multiplying the two deviations.

Equation (1) is the correlation coefficient formula, where x and y denote two variables, $x_i, y_i, i = 1, 2, \dots, n$; n denotes a total of n groups of data, \bar{x} and \bar{y} denote the averages of the above two variables; and r is in the range of -1 – 1 . A value of $|r|$ closer to 1 indicates a strong correlation, whereas a value closer to 0 indicates a weak correlation.

$$r = \frac{\sum_{i=1}^n (x_i - \bar{x})(y_i - \bar{y})}{\sqrt{\sum_{i=1}^n (x_i - \bar{x})^2 \sum_{i=1}^n (y_i - \bar{y})^2}} = \frac{n \sum_{i=1}^n x_i y_i - \sum_{i=1}^n x_i \cdot \sum_{i=1}^n y_i}{\sqrt{n \sum_{i=1}^n x_i^2 - \left(\sum_{i=1}^n x_i\right)^2} \cdot \sqrt{n \sum_{i=1}^n y_i^2 - \left(\sum_{i=1}^n y_i\right)^2}} \quad (1)$$

The correlation analyses of the nine electrical condition monitoring parameters in the smart electricity system were carried out, and the results are shown in Table 1.

Table 1
Correlation analysis results of key variables.

	I_a	I_{nn}	T_1	T_2	T_3	T_4	U_a	U_b	U_c
I_a	1	0.856	-0.52	-0.52	-0.52	-0.52	-0.61	-0.62	-0.63
I_{nn}	0.826	1	0.066	0.07	0.067	0.067	-0.69	-0.69	-0.69
T_1	-0.05	0.068	1	1	0.99	0.994	-0.15	-0.12	-0.13
T_2	-0.05	0.07	1	1	0.99	1	-0.16	-0.13	-0.13
T_3	-0.05	0.068	0.98	0.99	1	0.995	-0.16	-0.13	-0.13
T_4	-0.05	0.068	1	1	0.995	1	-0.16	-0.13	-0.14
U_a	-0.60	-0.69	-0.15	-0.16	-0.16	-0.15	1	0.995	0.99
U_b	-0.61	-0.69	-0.15	-0.14	-0.15	-0.13	0.99	1	0.99
U_c	-0.63	-0.69	-0.15	-0.14	-0.14	-0.134	0.99	0.99	1

From Table 1, it can be seen that the A-phase voltage and three-phase current are negatively related to the residual current. Because the voltage collected here is the circuit end voltage, by the full Ohm's law, the end voltage is negatively correlated with the circuit current. The absolute values of the correlation coefficients I_{nn} , U_a , U_b , U_c , and I_a are greater than or equal to 0.69, indicating a strong correlation. The values of T_1 , T_2 , T_3 , and T_4 are small and close to 0, indicating a weak correlation. Therefore, from the results of the above analysis, we chose I_{nn} as the output of the network and the factors affecting I_{nn} , i.e., three-phase voltage (U_a , U_b , and U_c) and A-phase current (I_a), as input values. These data are divided into a training set and a test set, where the training set is used to train the neural network model and the test set is used to calculate the model error accuracy.

2.2 Grey neural network model

The grey model (GM), a key principle of the proposed system, is briefly outlined as follows. GM represents systems that contain both known and unknown information.^(18–20) GM constitutes a forecasting methodology designed to address scenarios characterized by incomplete or uncertain information. By manipulating data sequences to reveal underlying trends and patterns, this method primarily employs cumulative data generation to mitigate randomness, subsequently establishing a grey differential equation model to project future behaviors. Such a model offers effective predictions in cases of limited data availability, rendering it particularly applicable to fields where data scarcity impedes conventional forecasting efforts, including economic forecasting, technological progression, and environmental change analysis. In this paper, we use GM (1, 1) to denote the grey prediction model of first-order 1 variable. GM (1, 1) is constructed from the new series calculated by accumulating the original data series. The modeling steps are as follows.

(a) Compute the cumulative sequence $x(1)$ from the original data sequence $x(0)$.

(b) To construct the model equation $\frac{dx}{dt} + ax = u$ and find a and u , create the matrix B , y . Let

$$U = \begin{bmatrix} a \\ u \end{bmatrix}, \text{ where}$$

$$B = \begin{bmatrix} -\frac{1}{2}[x^{(1)}(2) + x^{(1)}(1)] & 1 \\ -\frac{1}{2}[x^{(1)}(3) + x^{(1)}(2)] & 1 \\ \vdots & \vdots \\ -\frac{1}{2}[x^{(1)}(N) + x^{(1)}(N-1)] & 1 \end{bmatrix}, y = BU. \quad (2)$$

(c) Calculate the inverse matrix $(B^T B)^{-1}$.

(d) Calculate the estimates \hat{a} and \hat{u} from the least squares estimate $\hat{U} = \begin{bmatrix} \hat{a} \\ \hat{u} \end{bmatrix} = (B^T B)^{-1} B^T y$.

(e) Calculate the fitted value $x^1(i)$ using the time response equation and then reduce it using the post-subtraction operation (the inverse process of the cumulative operation), i.e., $x^0(0) = x(i) - \hat{x}(i-1), (i = 2, 3, \dots, N)$.

Model accuracy test: After determining the prediction model, it is necessary to verify the model to determine whether it is reasonable, and then make predictions.^(21,22) There are three general methods to test the accuracy of GM: relative error size test,⁽²³⁾ correlation test,⁽²⁴⁾ and a *posteriori* difference test.⁽²⁵⁾ In this paper, the *a posteriori* difference test is adopted, and the formula for calculating the *a posteriori* difference is

$$C = S_2 / S_1, \quad (3)$$

which is the ratio of the absolute error series standard deviation S_2 to the original series standard deviation S_1 .

$$P = P \left\{ \left| \Delta^{(0)}(i) - \bar{\Delta}^{(0)} \right| < 0.6745 S_1 \right\}. \quad (4)$$

Equation (4) represents the small error probability, where the standard deviation of the original academic series is

$$S_1^2 = \frac{1}{n} \sum_{k=1}^n [x^{(0)}(k) - \bar{x}]^2. \quad (5)$$

The standard deviation of the absolute error series can be calculated as

$$S_2^2 = \frac{1}{n} \sum_{k=1}^n [e(k) - \bar{e}]^2. \quad (6)$$

In GM (1, 1), the indicators C and P are important for the *a posteriori* difference test. The smaller the indicator C , the better. A smaller C means that it has a larger denominator S_1 or a smaller numerator S_2 . A larger S_1 suggests that the original data exhibits significant variance, i.e., the original data is highly dispersed; a smaller S_2 indicates that the variance of the residuals is small, i.e., the residuals are less dispersed. The smaller C indicates that although the original data is highly dispersed, the dispersion of the difference between the computed value and the actual value obtained from the model is small. The error probability P indicates the error probability level; the closer P is to 1, the higher the model prediction accuracy. The standard error accuracy control is shown in Table 2.

The data for the future time period to be predicted is obtained through GM and the data of a known time period is collected by the system. The above data is input to a neural network model for training and prediction and, finally, the prediction results that fully consider the historical information are obtained.

Next, we describe the neural network algorithm used in this study. The neural network is still widely used because of its simple structure, excellent nonlinear mapping, and adaptive and fault-tolerant capabilities.^(26–28) It consists of three parts: input layer, hidden layer, and output layer. The structure of the neural network is shown in Fig. 4.

Table 2
Standard error precision.

	Posterior error ratio C	Error probability P
I (good)	<0.35	≥ 0.95
II (qualified)	<0.50	≥ 0.80
III (barely qualified)	<0.65	≥ 0.70
IV (disqualified)	≥ 0.65	<0.70

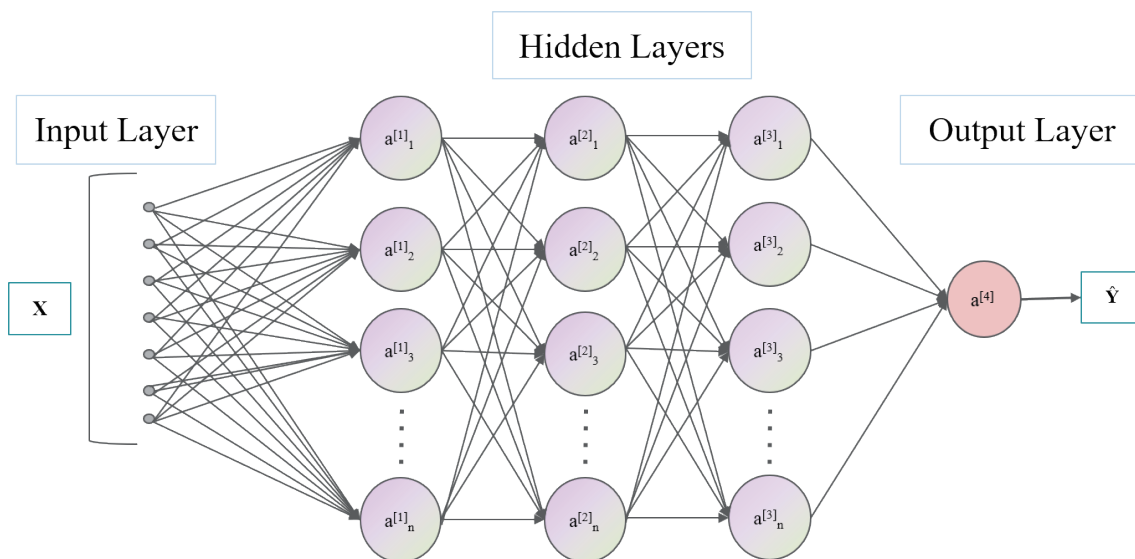


Fig. 4. (Color online) Structure of neural network.

The forward propagation process of the neural network is expressed as

$$a_j = \sigma \left(\sum_{i=1}^m \omega_{ij} x_i + b_j \right), (j = 1, 2, \dots, n), \quad (7)$$

$$y_k = \sigma \left(\sum_{j=1}^n \omega_{jk} a_j + b_k \right), (k = 1, 2, \dots, p), \quad (8)$$

$$\sigma(z) = \frac{1}{1 + e^{-z}}, \quad (9)$$

where m , n , and p are the numbers of neurons in the input, hidden, and output layers, respectively, x_i is the input vector, and y_k is the output vector. a_j is the vector of hidden layer outputs, w_{ij} and w_{jk} are weights, b_j and b_k are thresholds, and $\sigma(\bullet)$ is the activation function.

After forward propagation, the mean squared error loss function is established and the Levenberg–Marquardt algorithm is used to update the weights and optimize the objective function. The loss function expression is

$$Loss = \frac{1}{2} \sum_{k=1}^p (\hat{y}_k - y_k)^2, (k = 1, 2, \dots, p), \quad (10)$$

where \hat{y}_k is the output value obtained after one forward propagation and y_k is the true value.

The expression for the Levenberg–Marquardt algorithm used to update the weights and thresholds is

$$\begin{cases} \Delta W = -(J_1^T J_1 + uI)^{-1} J_1^T e \\ \Delta B = -(J_2^T J_2 + uI)^{-1} J_2^T e \end{cases}, \quad (11)$$

$$\begin{cases} W^{k+1} = W^k + \Delta W \\ B^{k+1} = B^k + \Delta B \end{cases}, \quad (12)$$

where W^k and B^k are the weight and threshold matrices of the k th iteration, respectively, J_1 and J_2 are Jacobi matrices, u is a trial parameter, and I is the unit matrix. $J_1^T J_1$ and $J_2^T J_2$ are used to approximate the Hessian matrix in the Gauss–Newton method, and $J_1^T e$ and $J_2^T e$ are used to represent the gradient in the gradient descent method.

The neural network model, designed for the electrical fire monitoring system, is rigorously trained using a dataset from the system, with its parameters finely tuned for accuracy and efficiency. The error precision is set at a highly precise 10^{-4} , ensuring that computational results are accurate to four decimal places, which is a critical factor for reliable predictions. In addition

to this precision, the model undergoes 500 learning iterations, a process essential for refining its predictive capabilities. During these iterations, the weights of the model are constantly updated, facilitating progressive reconstruction and optimization. This process is crucial for the model to effectively interpret complex data patterns. Moreover, the integration of a grey neural network, as shown in Fig. 5, combines grey system theory with neural network methodologies, enhancing the ability of the model to handle uncertainties and variabilities in data. This results in a robust model that offers both accuracy and resilience in predictions, which are crucial for effective monitoring and prevention in the realm of electrical fire safety.

The data are divided into training and test sets, in which the training and test set data are 27000 and 985 items, respectively. First, the grey prediction algorithm is used to obtain the input parameters of the prediction time period using the input parameter data in the training set. Then, the input parameter data in the training set and the grey prediction input parameter data are imported into the trained neural network model to output the residual current prediction. Finally, the mean squared error between the predicted and actual residual currents is calculated.

3. Experimental Results and Analysis

In this study, training sets encompassing nine electrical parameters were trained using a combined model to predict residual current values. The accuracy of the model was assessed by calculating the model error, which served as a metric for evaluating its efficacy. In previous correlation analyses, a close relationship was found between the three-phase voltage and the

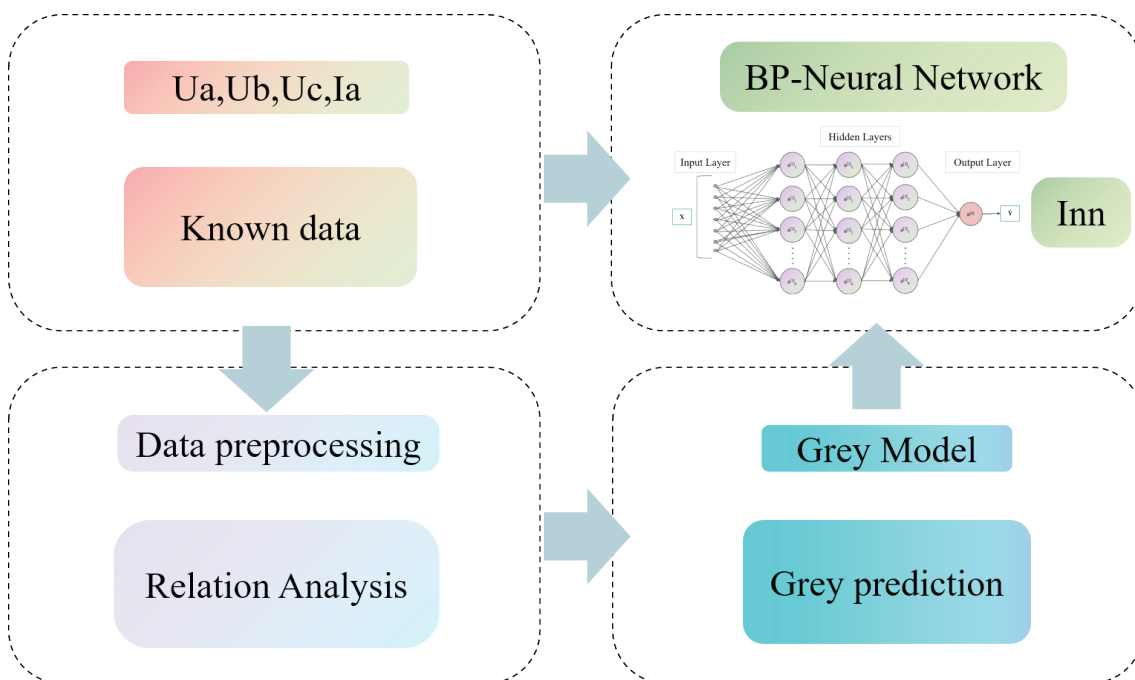


Fig. 5. (Color online) Recognition process of combinatorial models.

A-phase current with the residual current I_{nn} . Consequently, the grey prediction algorithm was employed, and the calculated *a posteriori* difference and error probability were compared with the standard *a posteriori* difference and standard error probability. The results are shown in Table 3.

The error curve of the training model is depicted in Fig. 6. The horizontal coordinate indicates the number of training iterations (unit/time), whereas the vertical coordinate denotes the training error. A training error approaching 0 suggests improved training outcomes. It can be observed from the curve that, at 500 iterations, the training of the model concludes, and the resulting training error approaches 0, indicating favorable training results.

From Fig. 6, it can be seen that as the number of training times increases, the model error decreases and the accuracy increases, which indicates that the model is applicable.

Calculation based on Eq. (10) gives the result of the mean squared error of residual current in units of mA². The error range is 0.18–3.21%.

In Fig. 7, the residual current predicted using the combined grey prediction and neural network model is compared with the actual value. The vertical coordinate of the graph denotes the residual current, whereas the horizontal coordinate signifies the number of datasets. The application of the algorithm, which combines GM with the neural network, has been found to significantly affect the trend and accuracy of prediction.

Table 3
Correlation factor accuracy of grey prediction.

	U_a/V	U_b/V	U_c/V	I_a/A
<i>a posteriori</i> difference C	0.435	0.427	0.495	0.586
Error probability P	0.806 (qualified)	0.826 (qualified)	0.804 (qualified)	0.912 (qualified)

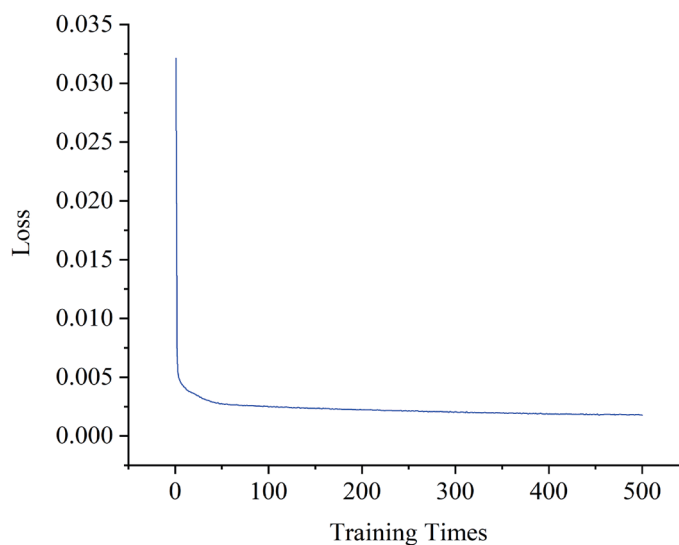


Fig. 6. (Color online) Error of training model.

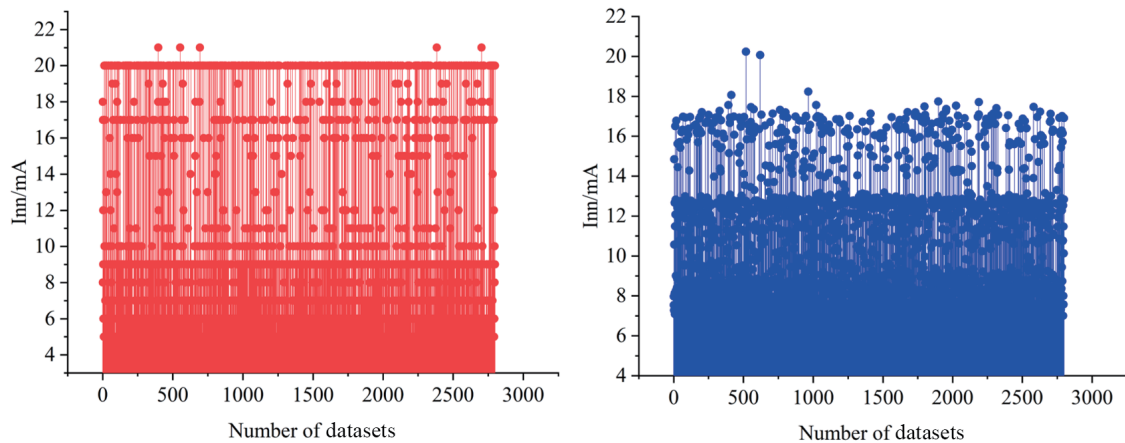


Fig. 7. (Color online) Results of model training (true vs predicted values).

4. Conclusion

A residual current prediction method based on the grey neural network was introduced in this study. Initially, electrical data were analyzed and processed to select model parameters. Subsequently, the grey prediction algorithm was employed to obtain the input parameter data for the specified prediction time period. All input parameter data were then fed into the trained neural network model, resulting in the predicted residual current. Finally, the training error and error accuracy of the prediction model were computed. The training model, with its superior performance, is particularly relevant in the context of integrating optimization and sensor technologies for electrical fire safety. The robustness of this model has profound implications for enhancing the effectiveness of IoT-based monitoring systems. By utilizing advanced sensors to collect real-time data and applying this model to interpret such data, it becomes possible to proactively identify potential electrical hazards. This integration significantly boosts the capability to predict and prevent electrical fires, thereby markedly reducing their incidence. The use of IoT and sensors in this model not only elevates safety standards but also revolutionizes the approach to electrical fire risk assessment and prevention. Consequently, this study marks a substantial advancement in the field of electrical safety, opening new avenues for the application of technology in residential and industrial settings for safeguarding against electrical hazards.

References

- 1 Z. Li, F. Qiu, H. Yang, Y. Zhang, H. Chen, and Y. Du: IEEE/IAS 57th Industrial and Commercial Power Systems Technical Conf. (I&CPS) (IEEE, 2021) 1. <https://doi.org/10.1109/ICPS51807.2021.9416596>
- 2 M. A. Alqassim and N. N. Daeid: Case Stud. Fire Saf. **2** (2014) 28. <https://doi.org/10.1016/j.csfs.2014.10.001>
- 3 A. Asgary, A. Ghaffari, and J. Levy: Fire Saf. J. **45** (2010) 44. <https://doi.org/10.1016/j.firesaf.2009.10.002>
- 4 S. Xiao, S. Wang, L. Ge, H. Weng, X. Fang, Z. Peng, and W. Zeng: Sensors **23** (2023) 859. <https://doi.org/10.3390/s23020859>
- 5 M. Nakip, C. Guzelis, and O. Yildiz: IEEE Access **9** (2021) 84204. <https://doi.org/10.1109/ACCESS.2021.3087736>
- 6 J. Baek, T. J. Alhindi, Y. S. Jeong, M. K. Jeong, S. Seo, J. Kang, and Y. Heo: IEEE Sensors J. **21** (2021) 27982. <https://doi.org/10.1109/JSEN.2021.3124266>

- 7 G. D. Georgiev, G. Hristov, P. Zahariev, and D. Kinaneva: 28th National Conf. Int. Participation (TELECOM). Sofia, Bulgaria: (IEEE, 2020) 57. <https://doi.org/10.1109/TELECOM50385.2020.9299566>
- 8 L. Wu, L. Chen, and X. Hao: Information **12** (2021) 59. <https://doi.org/10.3390/info12020059>
- 9 P. Liu, P. Xiang, and D. Lu: Neural Comput. Appl. **35** (2023) 25275. <https://doi.org/10.1007/s00521-023-08709-4>
- 10 H. Bian, Z. Zhu, X. Zang, X. Luo, and M. Jiang: Fire **5** (2022) 212. <https://doi.org/10.3390/fire5060212>
- 11 A. Gaur, A. Singh, A. Verma, and A. Kumar: IETE J. Res. **68** (2022) 1. <https://doi.org/10.1080/03772063.2022.2088626>
- 12 N. Xu, N. Ding, L. Liu, F. Zaïri, W. Guo, F. Li, and L. Chen: Mater. Test. **65** (2023) 844. <https://doi.org/10.1515/mt-2022-0423>
- 13 T. H. Cheng, C. H. Chen, C. H. Lin, B. H. Sheu, C. H. Lin, and W. P. Chen: Electronics **12** (2023) 2123. <https://doi.org/10.3390/electronics12092123>
- 14 G. Liu, J. Miao, X. Zhao, Z. Wang, and X. Li: J. Electr. Eng. Technol. **17** (2022) 2003. <https://doi.org/10.1007/s42835-022-01011-8>
- 15 G. Liu, Z. Wang, X. Li, C. Yue, and W. Li: IEEJ Trans. Electr. Electron. Eng. **16** (2021) 1165. <https://doi.org/10.1002/tee.23414>
- 16 E. Ghaderpour, S. D. Pagiatakis, and Q. K. Hassan: Applied Sciences **11** (2021) 6141. <https://doi.org/10.3390/appl1136141>
- 17 R. R. Singh, S. M. Yash, S. C. Shubham, V. Indragandhi, V. Vijayakumar, P. Saravanan, and V. Subramaniaswamy: Future Gener. Comput. Syst. **112** (2020) 884. <https://doi.org/10.1016/j.future.2020.06.032>
- 18 F. E. Sapnken: Grey Systems: Grey Syst. Theory Appl. **13** (2023) 406. <https://doi.org/10.1108/GS-09-2022-0100>
- 19 K. Shaju, S. Babu, and B. Thomas: Eng. Appl. Artif. Intell. **123** (2023) 106243. <https://doi.org/10.1016/j.engappai.2023.106243>
- 20 K. Zhang, K. Yin, and W. Yang: Expert Syst. Appl. **223** (2023) 119889. <https://doi.org/10.1016/j.eswa.2023.119889>
- 21 Y. Feng, Y. Dang, J. Wang, and Y. An: ISA Trans. **135** (2023) 398. <https://doi.org/10.1016/j.isatra.2022.09.014>
- 22 M. Dun, Z. Xu, L. Wu, and Y. Chen: J. Comput. Appl. Math. **415** (2022) 114460. <https://doi.org/10.1016/j.cam.2022.114460>
- 23 Z. Öztürk, H. Bilgil, and Ü. Erdinç: Hacettepe J. Mathematics and Statistics **51** (2022) 308. <https://doi.org/10.15672/hujms.939543>
- 24 R. Yao, S. Jin, C. Wei, and J. Kong: Discrete Dyn. Nat. Soc. **2022** (2022) 2022. <https://doi.org/10.1155/2022/2182748>
- 25 S. Yan, Q. Su, Z. Gong, and X. Zeng: Expert Syst. Appl. **197** (2022) 116691. <https://doi.org/10.1016/j.eswa.2022.116691>
- 26 Z. Cui, L. Kang, L. Li, L. Wang, and K. Wang: Renewable Energy **198** (2022) 1328. <https://doi.org/10.1016/j.renene.2022.08.123>
- 27 A. Shafiq, A. B. Çolak, S. A. Lone, T. N. Sindhu, and T. Muhammad: Math. Methods Appl. Sci. (2022) 1. <https://doi.org/10.1002/mma.8178>
- 28 J. Fei and L. Liu: IRE Trans. Ind. Electron. **69** (2021) 8366. <https://doi.org/10.1109/TIE.2021.3106007>

About the Authors



Guoyu Sun received his B.S. degree from Northeast Petroleum University, China, in 2007 and his M.S. degree from Harbin University of Science and Technology, China, in 2010. Since 2010, he has been an R&D engineer at Microsoft (China) Co., Ltd. His research interests are in machine learning and sensor detection. (sungy618@163.com)